Theoretical Calculation of Different Ion Surface Interaction Parameters of Si Target

Sarwar H. Ali*, S. R. Saeed**

* Department of Physics , Faculty of Science and Educational Science, Sulaimani, Kurdistan region, Iraq, E_mail: sarwar.hasan77@yahoo.com
** Department of General Science, Faculty Education - Chamchamal, University of Sulaimani, Chamchamal, Kurdistan region, Iraq, E_mail:salah.saeed@univsul.net.

Received: 25 Nov. 2013,Revised: 14 Jan. 2014, Accepted : 27 Jan. 2014
Published online: 26 Mar. 2014

Abstract:

Longitudinal projected range, energy losses, and sputtering yield are calculated of silicon target that bombarded with inert ion gases such as He, Ne, Ar, Kr, and Xe using SRIM package. Obtained results show increasing of longitudinal projected range with ion energy and decreasing with incident ion mass. The energy losses originated by the nuclear and electronic depending on ion ranges, generally at low ion energy the nuclear stopping power is dominated in comparison with the electronic stopping power, and the range of domination varies with changing ion species. Further, the sputtering yield founded, increasing with ion energy up to maximum value then tending to decrease, as well as it increases with increasing ion incident angle and decreases with decreasing ion mass.

Keywords: sputtering; ion range; energy loss; ion bombardement.

1. Introduction:

When a solid surface bombarded with energetic ions, many processes are initiated due to the collision of the incident ions with the nuclei and electrons of the material atoms [1], and it gives rise to a variety of physical and chemical phenomena [2]. During the bombarding of a solid surface with energetic ions, surface material will be removed, this mechanism is called sputtering. Grove first observed sputtering in a DC gas discharge tube in 1852 [3]. A target atom becomes sputtered when it displaced near the target surface and has a trajectory away from the surface and has sufficient kinetic energy so that it no longer interacts with other target surface atoms (overcoming the surface binding energy, U_o), thus escaping and becoming a gas phase sputtered atom.

Chemical sputtering may take place, if the bombarding particles are not noble gas atoms or ions. Chemical sputtering refers to the process where the energetic particles implanted in the target react chemically with the surface atoms and alter their ejection behavior [4].

Sputtering is typically quantified by the total sputter yield, Y, and is defined as the mean number of atoms removed from the surface of a solid per incident particle. Experimentally the sputtering yield depends on the incidence angle [5-7], ion energy [8-10], ion mass [11], and ion fluence [12], substrate atomic number [3], target crystallinity [3] and temperature [13].

When an energetic ion penetrates a solid, it undergoes a series of collisions with the atoms

and electrons in the target. In these collisions the incident particles gradually lose energy in many small steps. The Stopping power of a medium for a particle is a measure of the average energy loss per unit path length of the particle designated by dE/dx due to interactions with atoms in the medium, it depends on the energy and mass of the ions as well as on the properties of the material it passes.

The stopping power can be divided into nuclear and electronic stopping terms. Hence, the differential energy loss or stopping power or slowing down force of a layer dx of the target can be expressed as a sum of the nuclear (n) and electronic (e) contributions [14]:

$$\frac{dE}{dx} = \left(\frac{dE}{dx}\right)_n + \left(\frac{dE}{dx}\right)_e \qquad (1)$$

Nuclear stopping power is the energy lost by a moving particle due to elastic collisions per unit length traveled in the target (between the incident ion and atoms), energy will transfer by the ion to the target nuclei, and this collision type involves large discrete energy losses and significant angular deflection of the trajectory of the ion. And it produces lattice disorder by the displacement of atoms from their positions in the lattice. Nuclear stopping predominates for low E and high Z_1 [15].

Electronic stopping power is the energy lost by a moving particle due to inelastic collisions per unit length traveled in the target; energy will transfer by the ion to the target electrons. Inelastic term refers to the fact that the collision may result in excitation of the electrons of the target atoms and in excitation of the electrons clouds of the incident ions. Electronic stopping takes over high E and low Z_1 [15], this energy loss process reduces the energy of the moving atom, but does not change the direction of a moving atom. This effect is smaller than the elastic loss at low energies but becomes dominant at high energies [16].

When the incident ion loss its energy during the target penetration process, it is stop at a certain distance inside the solid target, the total distance that the projectile travels in coming to rest is called the range, *R*. the range of an energetic projectile with energy E_o is determined by the rate of energy loss along the path of the projectile:

$$R = \int_{E_o}^{0} \frac{1}{dE/dx}\, dE = \int_{E_o}^{0} \frac{dE}{NS(E)} \qquad (2)$$

Where E_o is the incident energy of the ion as it penetrates the solid. The sign *dE/dx* is negative, as it represents the energy loss per increment of path, although tabulated values are given as positive quantities [15]. Longitudinal projected range for a single ion (R_p), the projection of its R onto its incident trajectory vector, is the quantity most frequently used to describe depth for an ion implant. Where R_p for a distribution of ions in a target material is most commonly defined by convention, as the distance measured along the incident ion trajectory at which the highest concentration of implanted ions will be found [17].

The collision sequence and subsequent ion deflection, and the ion's total path length in coming to rest vary randomly from ion to ion. As a result, ions with the same energy, incident with the same angle onto the sample surface, and into the same material, do not necessarily come to rest in the same place. Hence, all ions of a given type and incident energy do not necessarily have the same range [15].

The main parameters governed the range or energy loss rate are the energy and atomic number of the ion Z_1 and atomic number of the substrate Z_2 if we exclude the effect to the orientation of the crystal lattice.

Simulation package:

The program that used was SRIM package. Stopping and Range of Ions in Matter (SRIM) is a group of computer programs which calculate interaction of ions with matter; the core of SRIM is a program Transport of ions in matter (TRIM). The programs were developed by James J.F. Ziegler and J.P. Biersack around 1983 . SRIM is group of programs that calculate the stopping range of ions in matter through quantum mechanical treatment of ion-atom collisions. It is a Monte-Carlo calculation which follows the ion into the target, making detailed calculations of the energy transferred to every target atom collision [18].

Results and Discussion:

A. Energy Losses

The variation of nuclear energy loss of the incident ions with energy of different masses (ion gases such as He, Ne, Ar, Kr, and Xe) on silicon target as shown in Fig. 1. Similar behavior have been observed for all ions interaction with target sample, where the nuclear stopping power goes through a maximum at specified energy then tend to decrease accompanied to the increase of electronic energy loss. Follow the maximum energy loss per unit length obtained at specified energy for each projectile: He (1.73 eV/A at 1keV), Ne(24.5 eV/A at 8keV), Ar (58.2 eV/A at 22.5keV), Kr (136 eV/A at 65keV), and Xe(213 eV/A at 150keV). The domination of nuclear energy loss extension to higher energy (more than 700 keV) in the case of Kr and Xe ions explains the role of the projectile mass.

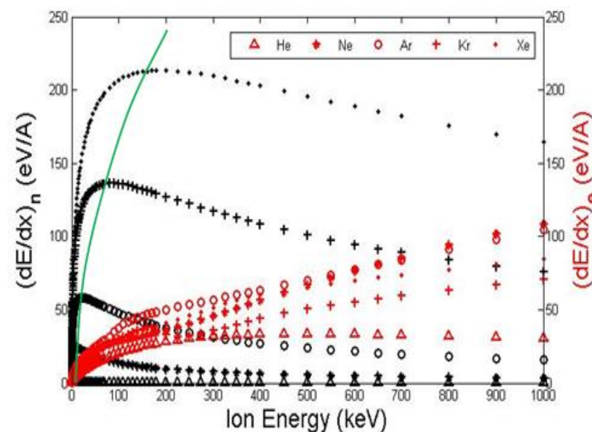

Fig.(1) The Nuclear and electronic energy loss of He, Ne, Ar, Kr, and Xe ion projectile in silicon target as a function of ion energy.

Except He the energy loss for ions Ne, Ar, Kr, and Xe in silicon as shown clearly in Fig. 1, mostly dominated by the nuclear energy loss for ion energies smaller than the mentioned energies, in these energy ranges, projectile energy loss occurs primarily through a series of nuclear collisions (elastic collision) between moving atoms (recoils) and other lattice atoms at rest. The target atoms are displaced from their original positions which correspond with some other effects include sputtering of surface atoms, generation and migration of point defects, amorphization of crystalline materials, and formation of surface layers with different properties relative to the bulk target. The interplay of various processes governs the evolution of morphological structures during irradiation.

In the case of faster moving ions, the energy losses inelastically by exciting the electrons of the target atoms (electronic stopping), the valence electrons are not free, but are so loosely bound that they can be considered to be free in the electronic energy loss. For higher ion energies (> 150 keV in the case of Ar ion projectile in Fig.1), the energy loss is dominated by electronic energy loss, due to

electronic interactions between the ion and the target. The energy acquired by the electrons is subsequently transferred to the atomic lattice via electron-phonon coupling, resulting in local lattice temperatures that can exceed several thousand Kelvin [19] which induces a cylindrically-shaped molten region of few nanometers around the ion track.

The total energy loss as a function of different ion species shown in Fig.2. The total energy loss increased with increasing ion mass. The higher the energy loss the higher the nuclear and electronic stopping crosses sections.

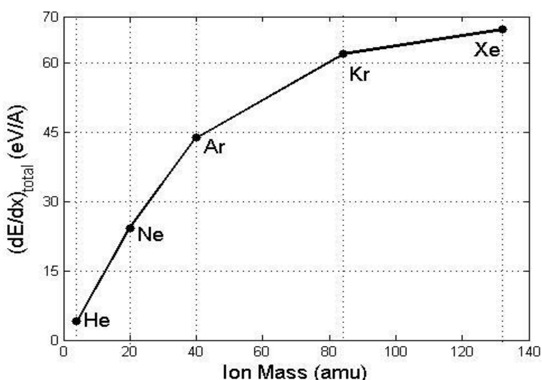

Fig. (2): Variation of the total energy loss of different incident ions (such as He, Ne, Ar, Kr, and Xe) on the silicon target with energy 2keV.

B. Longitudinal Projected Range

The variation of the longitudinal projected range of the (He, Ne, Ar, Kr, and Xe) ions incident on silicon surface as a function of ion energy at angle of 80° off-normal shown in the Fig.3, the higher the incident ion energy, the higher the penetration into the target. Also it was observed that the lighter ion characterizes by higher penetration.

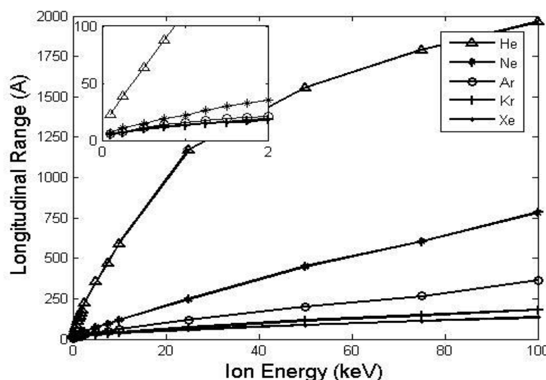

Fig. (3): Longitudinal projected range as a function of incident ion energy at angle of 80° off-normal for different ions irradiated silicon target. The insets on the left corners of the figures show the situations for low incident ion energy region.

Longitudinal projected range as a function of incident angle illustrated in Fig.4. It is indicates that by decreasing off-normal incident angle the ions penetrate to the deeper from the solid surface and vice versa.

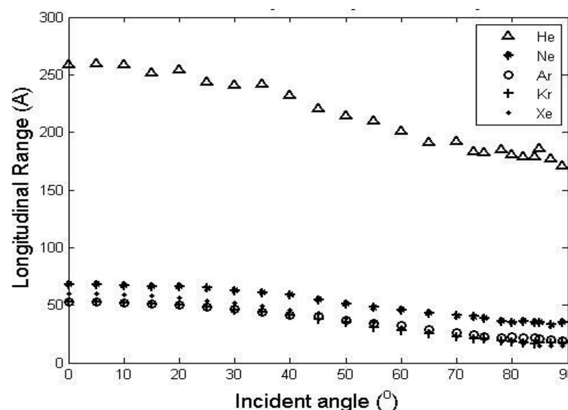

Fig. (4): Longitudinal projected range as a function of ion incident angle for different ions irradiated silicon target with energy of 2keV.

The variation of longitudinal projected range with the ion mass is shown in Fig.5, for lighter ion (He) the longitudinal projected range is higher than that of the heavy ion (Xe).

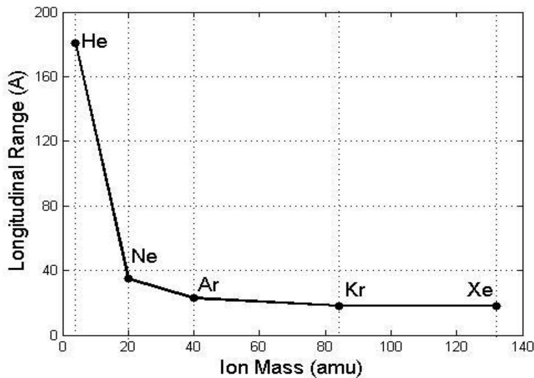

Fig. (5): Variation of longitudinal projected range with incident ion mass that bombarded Si target. Ion energy is 2keV and incident angle 80° off-normal.

The mean ion ranges generally increase with increasing ion energy and decrease with increasing ion mass. The higher the ion mass, the higher the energy losses, the lesser the penetration into the solid. In the wide incident ion energy range, the longitudinal projected range increases with increasing ion energy up to the maximum value then starts to decrease.

C. Sputtering Yield

For each target material there exist a threshold energy below which no sputtering occurs. Analytical theories predict that the dependence of Y on projectile energy, E, is given essentially by the energy dependence of the nuclear stopping power $S_n = (dE/dx)_n/N$, where N is the target atomic density, the results of Sigmund's theory is

$$Y(E) = 0.042\alpha S_n(E)/U_o \qquad (3)$$

Where U_o is the surface binding energy, and α a number which depends on the projectile/target mass ratio and the incidence angle, but is approximately independent of E at low projectile energies [6]. Fig.6 presents the sputtering yield dependence on the ion energy. At sufficiently low ion energy the energy transfer to recoils becomes lower than the surface binding energy (i.e. $E_{ion} < U_o$), so that sputtering is completely suppressed. When ion energy will be greater than the surface binding energy the target atoms will be start to sputter. Increasing ion energy increase sputtering yield until it reach the maximum value at certain ion energy, above that by increasing energy the sputtering yield decrease.

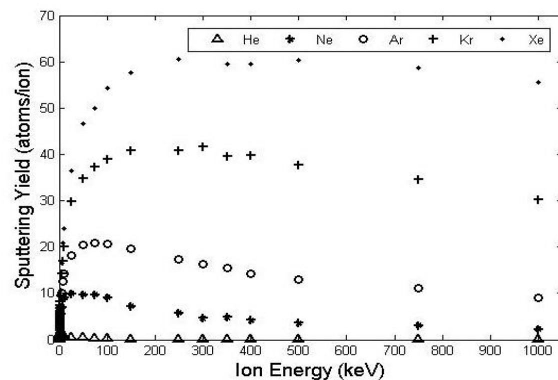

Fig. (6) The sputtering yield of silicon target as a function of the ion energy at incident angle of 80° off-normal of different ions (He, Ne, Ar, Kr, and Xe).

At the lower energies a large majority of interactions are very near the surface [8], by increasing energy the projectile penetrates deeper in to the target and only a small fraction of energy is dissipated in collision near the surface, at a certain large energy the beam penetrates deeper into the sample, sputtered atoms is not ejected from the near surfaces (subsurfaces) but remains within it.

The sputtering yield of silicon target atoms increases with the off-normal incidence angle of the ion beam as shown in Fig.7. The maximum yield appear in the certain angle (depend on the ion type and its energy), while it decreases rapidly for larger angles. The sputter

yield of Si and SiO_2 for example increases by a factor of seven to eight times in going from normal incidence to an angle of $75^o – 85^o$ [20].

For a certain ion the maximum of the angular dependence shifts to larger angles of incidence with increasing projectile energy and the probability of collision cascade decreases due to the participation of a few layers in the process [16].

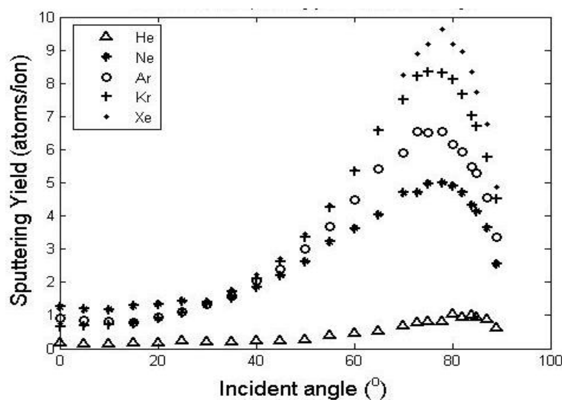

Fig. (7): Angular dependence of sputtering yields for bombardment of silicon with argon ion at 2keV projectile energy.

By varying the incident angle, sputter re-deposition can be controlled which affect the surface morphology. The projectile loses a large share of its energy near the surface region of the target as the angle of incidence with respect to surface normal increases. For angles near to the normal, the incident ion penetrates deeper to the target and only a smaller fraction of the energy is dissipated in collisions bear the surface. The subsequence decline is caused by rapid increase in the reflection coefficient as the direction of incidence approaches the glancing one [10].

Material removal rate can also be changed by varying the overlap of the collision cascades, which occur in the sample material during ion bombarding. When the ion beam hits the sample surface, collision cascades within the sample take place, resulting in some material sputtered out of the sample surface. Fig.8 shows schematic of collision cascades occurring within the target material as the beam incident on the target. Higher sputtering rate occurs when the collision cascades overlap than when collision cascades do not overlap. This enhancement occurs due to the increase in collision cross-section when the collision cascades overlap. [21]

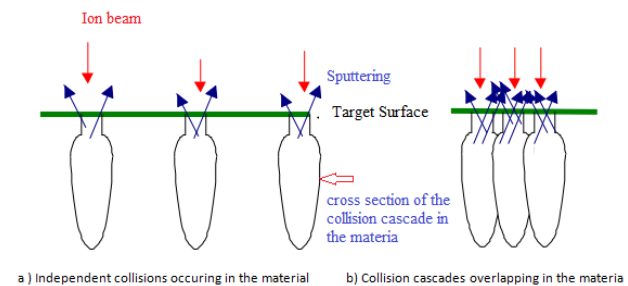

Fig. (8): Overlapping collision cascades within the material lead to enhancement of Sputtering.

The sputtering yield as functions of the incident ion mass for energy 2keV at incidence angle of 80° represents in Fig.9. It is seen that the variation of ion mass (He:2, Ne: 20, Ar: 40, Kr: 84, and Xe: 132 in amu.) act on the sputtering yield which attribute to the fact that with increasing ion mass the amount of energy deposition increases and also the collision cascade became larger correspond the wider cross section area of interaction, clearly appear that the sputtering yield due to He ion irradiation is significantly lower than those with higher mass such as Kr and Xe ions for the same irradiation parameters such as ion incident angle, ion energy and target sample.

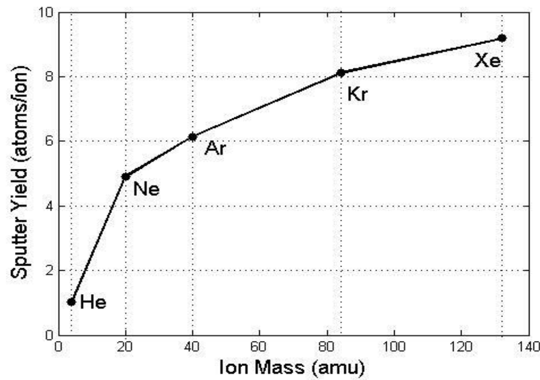

Fig. 9 Sputtering yield of silicon target atoms as a function of the incident ion mass at incident energies of 2 keV and angle of 80° off-normal

Concluding Remarks:

Due to the interaction of different ion species with the Si target, the following remarks have been calculated:

- Longitudinal projected (ion) range directly proportional with the ion energy and the abrupt have been observed especially in the case of Kr and Xe. It decreases with increasing incident angle.

- Energy loss (electronic and nuclear) increase with increasing ion energy, approaches the maximum value then tend to decrease, at different range of energy also increase with increasing ion mass, especially in ballistic process in the low energy range.

- Sputtering yield varies with ion energy; goes through maximum then tend to decrease depending on the ion mass. The higher the ion mass the higher the sputtering yield.

Acknowledgments

The Authors acknowledge the Faculty of Science and Educational Science, department of physics for supporting our work.

References

[1]. Marina, Ines Cornejo (2011) "Pattern Formation on Si surfaces by low-energy ion beam erosion", *ph.D. dissertation*, university of Saarlandes, Saarbrucken/ Leipaig.

[2]. Saeed, Salah R. (2008) "Nanometer-Scale Patterning of A_{III}-B_V Semiconductor and Alkali Halide Surfaces by Low Energy Ion Bombardment", *Ph.D dissertation*, Jagiellonian University, Kraków.

[3]. Wasa, Kiyotaka, Makoto Kitabataka and Hideaki Adachi (2004) *Thin film Materials Technology Sputtering of Compound materials*, William Andrew, Inc.

[4]. Nakles, Michael R. (2004) "Experimental and modeling studies of low-energy ion sputtering for ion thrusters", *M.Sc. thesis*, Virginia Polytechnic Institute and State University, United States.

[5]. Hu, A., and Hassanein A. (2012)"How surface roughness affects the angular dependence of the sputtering yield", *Nuclear Instruments and Methods in Physics Research Section B* 281: 15-20.

[6]. Oliva-Florio, A., Baragiola R.A., Jakas M.M., E.V. Alonso, and J. Ferron (1987) "Noble-gas ion sputtering yield of gold and copper: Dependence on the energy and angle of incidence of the projectiles", *Physical Revew B: Condensed Matter* 35: 2198-2204.

[7]. Bringa, E.M., and Johnson R.E. (2001) "Angular dependence of the sputtering yield from a cylindrical track", *Nuclear Instruments and Methods in Physics Research Section B* 180: 99-104.

[8]. Smith, P.C. and Ruzic D.N. (1998) "Low energy (10 to 700 eV) angularly resolved sputtering yields for D^+ on beryllium", *Nuclear fusion* 38: 673.

[9]. Samela, J., J. Kotakoski, K. Nordlund, andJ. Keinonen (2005) "A quantitative and comparative study of sputtering yields in Au", *Nuclear Instruments and Methods in Physics Research Section B* 239: 331—346.

[10]. Chini, T.K., S.R. Bhattacharyya, D. Basu, and J.P. Biersack (1994) "Angle of incidence variation of sputtering of germanium", *Radiation effects and defects in solids* 127: 349-355.

[11]. Yoshimura, Satoru, Kiyohiro Hine, Masato Kiuchi, Jun Hashimoto, Masaharu Terauchi, Yosuke Honda, Mikihiko Nishitani, and Satoshi Hamaguchi (2012) "Sputtering Yields of CaO, SrO, and BaO by Monochromatic Noble Gas Ion Bombardment", *Japanese Journal of Applied Physics* 51: 08HB02(1-3).

[12]. Hansen, Henri, (2005) "Pattern formation and evolution on Pt (111) by grazing incident ion bombardment", *Ph.D dissertation*, RWTH Aachen University, Germany.

[13]. Behrisch, Rainer, and Wolfgang Eckstein (1981) Sputtering by Particle Bombardment I, Springer-Verlag Berlin Heidelberg.

[14]. Gnaser, Hubert (1999) *Low-Energy Ion Irradiation of Solid*, Springer-Verlag Berlin Heidelberg.

[15]. Nastasi, Michael, James W.Mayer and James K.Hirvonen (1966) *Ion-Solid Interactions Fundamentals and Applications*, Cambridge University.

[16]. Behrisch, Rainer, and Wolfgang Eckstein (2007) *Sputtering by Particle Bombardment* , Springer-Verlag Berlin Heidelberg.

[17]. Giannuzzi, Lucille A., Brenda I. Prenitzer, and Brian W. Kempshall (2005) "Chapter 2: Ion-Solid Interactions" in *Introduction to Focused Ion Beams: Instrumentation, Theory, Techniques and Practice*, edited by Giannuzzi, Lucille A., and Fred A. Stevie, pp. 13-52. Springer science+Business Media Inc.

[18]. Ziegler, J.F. and J.P. Biersack. SRIM 2003 (Program and Documentation). http://www.srim.org

[19]. Toulemonde, M.,J.M. Costantini, Ch. Dufour, A. Meftah, E. Paumier, and F. Studer, (1996) "Track creation in SiO_2 and $BaFe_{12}O_{19}$ by swift heavy ions: a thermal spike description",*Nuclear Instruments and Methods in Physics Research Section B: Beam Interactions with Materials and Atoms* 116: 37- 42.

[20]. Santamore, D., K. Edinger, J. Orloff, and J. Melngailis, (1997) "Focused Ion Beam Sputter Yield Changes as a Function of Scan Speed", *Vacuum Science and Technology B*15, 2346.

[21]. Latif, Adnan, (2000) "Nanofabrication using focused ion beam", *Ph.D dissertation*, University of Cambridge, England, United Kingdom.